

# Combining Passivity-Based Control and Linear Quadratic Regulator to Control a Rotary Inverted Pendulum

Minh-Tai Vo <sup>1</sup>, Van-Dong-Hai Nguyen <sup>2</sup>, Hoai-Nghia Duong <sup>3</sup>, Vinh-Hao Nguyen <sup>4\*</sup>

<sup>1,4</sup> Faculty of Electrical and Electronics Engineering, Ho Chi Minh City University of Technology, VNU-HCM, Ho Chi Minh City, Vietnam

<sup>2</sup> Faculty of Electrical and Electronics Engineering, Ho Chi Minh City University of Technology and Education, Ho Chi Minh City, Vietnam

<sup>1</sup> School of Science, Engineering and Technology, Royal Melbourne Institute of Technology, Ho Chi Minh City, Vietnam

<sup>3</sup> School of Engineering, Eastern International University, Binh Duong Province, Vietnam

Email: <sup>1</sup> vmtai.sdh212@hcmut.edu.vn, <sup>2</sup> hainvd@hcmute.edu.vn, <sup>3</sup> nghia.duong@eiu.edu.vn, <sup>4</sup> vinhhao@hcmut.edu.vn

\*Corresponding Author

**Abstract**—In this manuscript, new combination methodology is proposed, which named combining Passivity-Based Control and Linear Quadratic Regulator (for short, CPBC-LQR), to support the stabilization process as the system is far from equilibrium point. More precisely, Linear Quadratic Regulator (for short, LQR) is used together with Passivity-Based Control (for short, PBC) controller. Though passivity-based control and linear quadratic regulator are two control methods, it is possible to integrate them together. The combination of passivity-based control and linear quadratic regulator is analyzed, designed and implemented on so-called rotary inverted pendulum system (for short, RIP). In this work, CPBC-LQR is validated and discussed on both MATLAB/Simulink environment and real-time experimental setup. The numerical simulation and experimental results reveal the ability of CPBC-LQR control scheme in stabilization problem and achieve a good and stable performance. Effectiveness and feasibility of proposed controller are confirmed via comparative simulation and experiments.

**Keywords**—Stabilization control; linear quadratic regulator; passivity-based control; rotary inverted pendulum; combination.

## I. INTRODUCTION

RIP or Furuta pendulum system was first introduced in 1992 at Tokyo Institute of Technology by Katsuhisa Furuta and his colleagues. Swing up control scheme based on pseudo-state feedback is the first control strategy that Katsuhisa Furuta and his colleagues implemented successfully on RIP [1]. Professor K. Furuta and his colleagues continuously studied and published new results to scientific community in 2001, 2004, and 2006, respectively [56]–[58]. RIP is a single input multiple output system (SIMO) and under-actuated system (i.e., underactuated robots are those systems which have lower number of actuators

when compared to the number of degrees of freedom they possess). It is a good platform for outlining, testing, validation for control engineers, researchers to qualify control approaches.

After 30 years from the first time of introducing to scientific community, RIP is still used to validate the control techniques. A number of control strategies have been applied for RIP such as optimizing time of swing-up to control of RIP [2], safe manual control strategy for RIP [3], virtual holonomic constraint for stabilization control [4], research of limit cycle elimination in RIP and pendubot [5], nonlinear sliding mode control methodology [6], memory output-feedback integral sliding mode control [7], a research related to Bayesian Optimization [8]. Apart from that research has been completed on the use of intelligence control which are paraconsistent neural network for RIP identification [9], deep neural network [10]–[12], [65], fuzzy logic control (FLC) [13], [14]. Besides, soft computation such as genetic algorithm (GA) [13], [14], [16]–[18], practical swarm optimization [15], gravitational search algorithm (GSA) [16], seeker optimization algorithm (SOA) [16], Teaching-learning based optimization (TLBO) [16]. Adaptive control technique has been qualified on RIP [19]–[21].

In addition, some researchers combine two or three control strategies for validation on RIP system. For instance, linear quadratic regulator associates with neural network for improving the responses [22], Lyapunov-base controller and linear PD controller [23], LQR-FLC and LQR-PID [24]–[26], backstepping sliding mode controller [27], fuzzy-sliding mode controller [28]. Moreover, swing-up and trajectory tracking are problems that many researcher focus on studying and using RIP for validation their proposed control schemes. Swing-up



controller is used to swing an inverted pendulum from original position (stable position) to vertical upright position (unstable position). A few authors concentrate on addressing the swing-up control of RIP such as [48], [56], [57], [59]–[64]. Trajectory tracking control is one of topic to study in control engineering [66]–[69]. Besides, a few authors use programmable logic controller (PLC) to control of RIP such as [70]–[73].

PBC is a nonlinear control methodology, can handle the performance of system, not just stability. The main point of PBC is a methodology which consists in controlling a system with the aim at making the closed loop system, passive [29]. Although, PBC was first introduced in 1980s [30], this control strategy still develops and many studies have been done by using this methodology [39]–[42]. This method has been qualified in some studies such as robust PBC for active suspension system [31], application of PBC for single-phase cascaded H-Bridge grid-connected photovoltaic inverter [32], validation of PBC for three-level photovoltaic inverter to mitigate common-mode resonant current [33]. Besides, researchers have ideas like combining PBC with other control strategies. For example, passivity-based sliding mode control [34]–[37], passivity-based sliding mode observer [37], passive-based adaptive robust super-twisting nonlinear controller [38]. LQR technique is a popular linear control scheme, the principle of this method can be referred to [22]. LQR approach has been studied in many research belong to different fields [43]–[47].

Since RIP system is a nonlinear and unstable system, selecting such wide ranges of the gains in the digital-deployment environment hinders its applicability [22]. As a sequence, in this work, we focus on combining two control strategies including PBC and LQR for stabilizing a RIP system at vertical upright position. Control scheme is structured with PBC control signal and LQR control signal. Advantage of LQR is well-stabilizing the closed-loop system arbitrarily around equilibrium point. Meanwhile, nonlinear control, such as PBC, has a wide working range due to feasibility of controller and stability proved by Lyapunov criteria. Hence, we propose a hybrid controller which can combine LQR and PBC to verify stabilization control of RIP. The main contributions of this manuscript are as follows:

- The hybrid controller is generated by combining PBC and LQR, on one hand, could support the stabilization process as the system is far from equilibrium point and, on the one hand, when RIP approaches the equilibrium posture, LQR takes responsibility for balancing inverted pendulum at upright position.
- Effectiveness and feasibility of CPBCLQR are investigated via comparative simulation and experiments.

The organization of paper is as follows: mathematical model of RIP and experimental setup are given in section 2. Section 3 introduces passivity theory, passivity of RIP, theory of LQR technique, PBC and LQR design, combination of PBC and LQR. Numerical simulation, experimental results and com-

ments are drawn in section 4. Finally, conclusion and final remarks are presented in section 5 of this paper.

## II. ROTARY INVERTED PENDULUM WORKING PRINCIPLE, DYNAMIC MODEL AND EXPERIMENTAL SETUP

### A. Rotary Inverted Pendulum Working Principle and Dynamic Model

RIP is an under-actuated robot that has two degrees of freedom (2-DOF). Basic structural components consist of arm, pendulum, and DC servo motor. There are two angles shown in Fig. 1, one for arm and one for pendulum. DC servo motor's shaft with encoder is attached to arm one, which moves horizontally. Pendulum is connected with arm via encoder, which moves rotational. Expectation objective of this system is to control pendulum one stabilize at vertical upright position (equilibrium point). The angle of arm is denoted as  $\theta_1$  and the angle of pendulum is denoted as  $\theta_2$ .

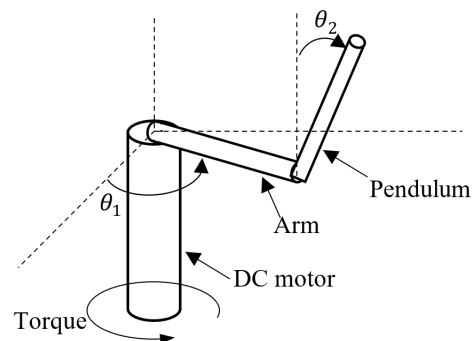


Fig. 1. Rotary inverted pendulum model

First of all, information of parameters of system and their value are introduced in Table I. The value of those parameters are measured and identified based on real time model that shown in Fig. 3.

TABLE I. PARAMETERS OF SYSTEM AND VALUE

Nr.	Symbol	Value	Unit	Parameter
1	$m$	0.027	kg	Mass of pendulum
2	$L_1$	0.205	m	Length of arm
3	$J_1$	0.0019	kgm <sup>2</sup>	Inertial moment of arm
4	$L_2$	0.328	m	Length of pendulum
5	$J_2$	0.0046617	kgm <sup>2</sup>	Inertial moment of pendulum
6	$C_1$	0.025	Nm-s	Friction coefficient of arm
7	$C_2$	0.0017	Nm-s	Friction coefficient of pendulum
8	$g$	9.81	m/s <sup>2</sup>	Gravitation acceleration

Equations of motion are described in Eq. (1) [48]. The dynamic model is affected by many factors such as Centrifugal

forces, Coriolis forces, Gravitational forces, etc. Motion equations are given in Eq. (1)

$$M(\theta)\ddot{\theta} + C(\theta, \dot{\theta}) + G(\theta) = \begin{bmatrix} \tau \\ 0 \end{bmatrix} \quad (1)$$

where  $M(\theta)$  is inertia matrix,  $C(\theta, \dot{\theta})$  contains centrifugal/Coriolis terms and  $G(\theta)$  is the vector of gravity forces.

$$\begin{aligned} M(\theta) &= \begin{bmatrix} M_{11} & M_{12} \\ M_{21} & M_{22} \end{bmatrix} \\ C(\theta, \dot{\theta}) &= \begin{bmatrix} C_{11} & C_{12} \\ C_{21} & C_{22} \end{bmatrix} \\ G(\theta) &= \begin{bmatrix} G_1 \\ G_2 \end{bmatrix} \\ M_{11} &= J_1 + mL_1^2 + mL_2^2 \sin^2 \theta_2 \\ M_{12} &= M_{21} = -mL_1 L_2 \cos \theta_2 \\ M_{22} &= J_2 + mL_2^2 \\ C_{11} &= C_1 + \frac{1}{2} mL_2^2 \dot{\theta}_2 \sin 2\theta_2 \\ C_{12} &= mL_1 L_2 \dot{\theta}_2 \sin \theta_2 + \frac{1}{2} mL_2^2 \dot{\theta}_1 \sin 2\theta_2 \\ C_{21} &= -\frac{1}{2} mL_2^2 \dot{\theta}_1 \sin 2\theta_2 \\ C_{22} &= C_2, G_1 = 0, G_2 = mgL_2 \sin \theta_2. \end{aligned}$$

Note that the inertia matrix  $M(\theta)$  is symmetric matrix. Moreover,

$$\begin{aligned} M_{11} &= J_1 + mL_1^2 + mL_2^2 \sin^2 \theta_2 > 0 \\ \det(M(\theta)) &= J_1 J_2 + L_2^4 m^2 \sin^2(\theta_2)^2 + L_1^2 L_2^2 m^2 + \\ &+ J_1 L_2^2 m + J_1 L_2^2 m + J_2 L_2^2 m \sin(\theta_2)^2 + \\ &+ L_1^2 L_2^2 m^2 \cos(\theta_2)^2 > 0 \end{aligned} \quad (2)$$

Therefore,  $M(\theta)$  is positive definite for all  $\theta$

$$M(\theta) = M(\theta)^T \quad (3)$$

From Eq. (1) it follows that

$$N = \dot{M}(\theta) - 2C(\theta, \dot{\theta}) \quad (4)$$

is skew symmetric matrix for any  $(n \times 1)$  vector with  $N^T + N = 0$  and  $\dot{\theta}^T N(\theta, \dot{\theta}) \theta = 0$ . The skew symmetric matrix property plays an vital role for Lagrange dynamics. This property is used in establishing the passivity of RIP system is [29]:

$$z^T(N)z = 0 \quad \forall z \quad (5)$$

The RIP potential energy is defined in Eq. (6)

$$P = \frac{1}{2} mgL_2(1 + \cos \theta_2) \quad (6)$$

### B. Passivity of RIP

In this subsection, passivity of RIP is delivered. Total energy of RIP is given in Eq. (7)

$$H(\theta, \dot{\theta}) = \frac{1}{2} \dot{\theta}^T M(\theta) \dot{\theta} + P \quad (7)$$

Taking derivative of  $H(\theta, \dot{\theta})$  with respect to  $t$ , we obtain

$$\dot{H}(\theta, \dot{\theta}) = \dot{\theta}^T M(\theta) \ddot{\theta} + \frac{1}{2} \dot{\theta}^T \dot{M}(\theta) \dot{\theta} + \dot{\theta}^T G(\theta) = \dot{\theta}^T \tau \quad (8)$$

Integrating both sides of Eq. (8), we obtain Eq. (9):

$$\int_0^t \dot{\theta}^T \tau dt = H(t) - H(0) \quad (9)$$

Accordingly, RIP having  $\tau$  as control input and  $\dot{\theta}$  as output is passive. When  $\tau = 0$ , RIP in Eq. (1) has two equilibrium points, include  $(\theta_1, \dot{\theta}_1, \theta_2, \dot{\theta}_2) = (0, 0, \pi, 0)$  corresponding to downward position, is stable equilibrium position. For the remaining position,  $(\theta_1, \dot{\theta}_1, \theta_2, \dot{\theta}_2) = (0, 0, 0, 0)$  corresponding to the upright position, is unstable equilibrium position. Total energy of RIP is different between two equilibrium points. Total energy of each equilibrium points is described as follows

- $(\theta_1, \dot{\theta}_1, \theta_2, \dot{\theta}_2) = (0, 0, \pi, 0)$ . Total energy of RIP is  $H(\theta) = 0$ .
- $(\theta_1, \dot{\theta}_1, \theta_2, \dot{\theta}_2) = (0, 0, 0, 0)$ . Total energy of RIP is  $H(\theta) = 2\frac{1}{2}mgL_2$ .

The control target is to stabilize the RIP at vertical upright position, its unstable equilibrium point.

### C. DC Motor Model

Actually, the system is not yet completed. We observe that just the pendulum and rotary arm have been taken into account, but the DC servo motor has to implemented. Therefore, for the convenience of adjusting DC servo motor as well as applying control schemes to the real time experiment setup, authors transform the control signal from motor torque to voltage that is applied to DC motor by Eq. (10). Parameters of DC servo motor was carried out by previous study [81].

From the motion equations of RIP (1), the control input for mechanical system is motor torque  $\tau$ . This applied motor torque at the base of the rotary arm generated by the servo motor is described by Eq. (10). The motor can be simplified and expressed as shown in Eq. (10). This equation is implemented on MATLAB/Simulink model.

$$\tau = d_1 V - d_2 \dot{\theta}_1 \quad (10)$$

where  $d_1 = \frac{K_t}{R_m}$ ,  $d_2 = \frac{K_t^2}{R_m}$ ,  $\tau$  is the torque of DC motor,  $K_t$  is torque constant,  $V$  is input voltage,  $\dot{\theta}_1$  is motor angular velocity. Parameters of servo motor are provided in Table II.

TABLE II. SERVO MOTOR PARAMETERS

Nr.	Symbol	Value	Unit	Parameter
1	$R_m$	11.7356	$\Omega$	Armature resistance
2	$K_t$	0.0531	$\text{NmA}^{-1}$	Torque constant

#### D. Non-linear Dynamic Model

The non-linear dynamic model is used to model RIP plant in Matlab/Simulink software. Let  $x_1 = \theta_2$ ;  $x_2 = \dot{\theta}_2$ ;  $x_3 = \theta_1$ ;  $x_4 = \dot{\theta}_1$ . From equations (1) and (10), state-space equations in nonlinear form are given in Eq. (11) as follows:

$$\begin{aligned}
 \dot{x}_1(t) &= x_2; \\
 \dot{x}_2(t) &= f_1(x, t) + g_1(x, t)V; \\
 \dot{x}_3(t) &= x_4; \\
 \dot{x}_4(t) &= f_2(x, t) + g_2(x, t)V; \\
 y &= h(x)
 \end{aligned} \tag{11}$$

where  $y$  is output of system,  $e$  is input of system,  $x$  is state-space vector. Components  $f_1(x, t)$ ,  $f_2(x, t)$ ,  $g_1(x, t)$ ,  $g_2(x, t)$  are obtained as expressed below.

$$f(x) = [0 \quad f_1(x, t) \quad 0 \quad f_2(x, t)]^T;$$

$$g(x) = [0 \quad g_1(x, t) \quad 0 \quad g_2(x, t)]^T;$$

$$g_1(x, t) = \frac{mL_1L_2 \cos x_1}{J_2 + mL_2^2} g_2(x, t)$$

$$\begin{aligned}
 f_1(x, t) &= \frac{mL_1L_2 \cos x_1}{J_2 + mL_2^2} f_2(x, t) \\
 &+ \frac{1}{J_2 + mL_2^2} \left( \frac{1}{2} mL_2^2 x_4^2 \sin 2x_1 \right. \\
 &\left. - C_2 x_2 + mgL_2 \sin x_1 \right)
 \end{aligned}$$

$$\begin{aligned}
 g_2(x, t) &= d_1 \left( J_1 + mL_1^2 + mL_2^2 \sin^2 x_1 \right. \\
 &\left. - \frac{m^2 L_1^2 L_2^2 \cos^2 x_1}{J_2 + mL_2^2} \right)^{-1}
 \end{aligned}$$

$$\begin{aligned}
 f_2(x, t) &= \left( J_1 + mL_1^2 + mL_2^2 \sin^2 x_1 - \frac{m^2 L_1^2 L_2^2 \cos^2 x_1}{J_2 + mL_2^2} \right)^{-1} \\
 &\times \left\{ - \left( C_1 + d_2 + \frac{1}{2} mL_2^2 x_2 \sin 2x_1 \right. \right. \\
 &\left. \left. - \frac{m^2 L_1 L_2^2 x_4 \cos x_1 \sin 2x_1}{2(J_2 + mL_2^2)} \right) x_4 \right. \\
 &\left. - \left( mL_1 L_2 x_2 \sin x_1 + \frac{1}{2} mL_2^2 x_4 \sin 2x_1 \right. \right. \\
 &\left. \left. + \frac{C_2 mL_1 L_2 \cos x_1}{J_2 + mL_2^2} \right) x_2 + \frac{m^2 g L_1 L_2^2 \cos x_1 \sin x_1}{J_2 + mL_2^2} \right\}
 \end{aligned}$$

#### E. Linear Dynamic Model

Nominal linear state-space equation of RIP is obtained via Taylor expansion as  $x_1, x_2 \rightarrow 0$ . The model is then simplified and expressed as a linear state-space

$$\begin{cases} \dot{x} = Ax + BV \\ y = Cx + DV \end{cases} \tag{12}$$

where  $x$  is state vector (nx1),  $y$  is output vector (px1),  $u$  is control vector (mx1),  $A, B, C, D$  are matrices of system.

$$\begin{aligned}
 A &= \frac{1}{\lambda} \begin{bmatrix} 0 & \lambda & 0 & 0 \\ A_{21} & A_{22} & A_{23} & A_{24} \\ 0 & 0 & 0 & \lambda \\ A_{41} & A_{42} & A_{43} & A_{44} \end{bmatrix} \\
 B &= \frac{1}{\lambda} \begin{bmatrix} 0 \\ B_{21} \\ 0 \\ B_{41} \end{bmatrix} \\
 \lambda &= (J_1 + mL_1^2)(J_2 + mL_2^2) - (mL_1L_2)^2 \\
 A_{21} &= mgL_2(J_1 + mL_1^2) \\
 A_{22} &= -C_2(J_1 + mL_1^2) \\
 A_{23} &= 0 \\
 A_{24} &= -(mL_1L_2)(C_1 + d_2) \\
 A_{41} &= m^2gL_1L_2^2 \\
 A_{42} &= -C_2(mL_1L_2) \\
 A_{43} &= 0 \\
 A_{44} &= (J_2 + mL_2^2)(C_1 + d_2) \\
 B_{21} &= d_1(mL_1L_2) \\
 B_{41} &= d_1(J_2 + mL_2^2)
 \end{aligned} \tag{13}$$

$A, B$  matrices are calculated by substituting all parameters in Table I and Table II into Eq. (13). The input matrices,  $A, B, C, D$  are obtained as expressed in Eq. (14):

$$\begin{aligned}
 A &= \begin{bmatrix} 0 & 1 & 0 & 0 \\ 36.4628 & -0.0392 & 0 & -1.5058 \\ 0 & 0 & 0 & 1 \\ 23.3433 & -0.0251 & 0 & -2.9396 \end{bmatrix} \\
 B &= \begin{bmatrix} 0 \\ 1.1365 \\ 0 \\ 2.2186 \end{bmatrix} \\
 C &= \begin{bmatrix} 1 & 0 & 0 & 0 \\ 0 & 0 & 1 & 0 \end{bmatrix} \\
 D &= \begin{bmatrix} 0 \\ 0 \end{bmatrix}
 \end{aligned} \tag{14}$$

### III. CONTROLLER DESIGN

#### A. Passivity-based Control Scheme

Stabilizing RIP at  $\theta_i = \theta_d = [0, 0]^T$  ( $i=1,2$ ), we set

$$q = \theta_i - \theta_d; \dot{q} = \dot{\theta}_i \quad (15)$$

The control objective is to stabilize RIP at vertical upright position.  $\theta_d$  is selected as follows  $\theta_d = [0, 0]^T$ . Therefore,  $q = \theta_i$ ,  $\dot{q} = \dot{\theta}_i$ , and  $\ddot{q} = \ddot{\theta}_i$ . Note the  $q = 0$ ,  $\dot{q} = 0$  are not an open-loop equilibrium points.

From Eq. (15), the dynamics equations can be rewritten as follows Eq. (16)

$$M(\theta)\ddot{q} + C(\theta, \dot{\theta})\dot{q} + G(\theta) = \begin{bmatrix} V \\ 0 \end{bmatrix} \quad (16)$$

Feedback passivation control law is defined by

$$u_{PBC} = G(\theta) - \phi_p(q) + e \quad (17)$$

where  $\phi_p(0) = 0$ ,  $q^T \phi_p(q) > 0 \forall q \neq 0$

Based on Equations (15), (16), (17), equations of motion are obtained and expressed in Eq. (18)

$$M(\theta)\ddot{q} + C(\theta, \dot{\theta})\dot{q} + \phi_p(q) = \begin{bmatrix} e \\ 0 \end{bmatrix} \quad (18)$$

Storage function  $E_1$  is selected as follows:

$$E_1 = \frac{1}{2} \dot{q}^T M(\theta) \dot{q} + \int_0^q \phi_p(\psi) d\psi \quad (19)$$

Derivative of selected storage function  $E_1$  with respect to  $t$  in Eq. (19) becomes

$$\dot{E}_1 = \frac{1}{2} \dot{q}^T N \dot{q} - \dot{q}^T \phi_p(q) + \dot{q}^T e + \phi_p^T(q) \dot{q} \leq \dot{q}^T e \quad (20)$$

and

$$y = \dot{q} \quad (21)$$

RIP system is output strictly passive with  $y = \dot{q}$ . Zero-state observable property is validated, the new control input must be zero, i.e  $e = 0$

$$y = \dot{q}(t) \equiv 0 \Rightarrow \ddot{q}(t) \equiv 0 \Rightarrow \phi_p(q(t)) \equiv 0 \Rightarrow q(t) \equiv 0 \quad (22)$$

The passive control law is defined by

$$e = -\phi_d(\dot{q}) \quad (23)$$

where  $\phi_d(0) = 0$ ,  $\dot{q}^T \phi_d(\dot{q}) > 0 \forall \dot{q} \neq 0$

Control law of feedback control based on PBC is given by

$$u_{PBC} = G(\theta) - \phi_p(q) - \phi_d(\dot{q}) \quad (24)$$

We select  $\phi_p(q) = K_p q$  and  $\phi_d(\dot{q}) = K_d \dot{q}$  where  $K_p$ ,  $K_d$  are symmetric matrices and positive definite matrices,  $K_p = K_p^T > 0$ ,  $K_d = K_d^T > 0$

#### B. LQR Approach

The objective of LQR control scheme is to define feedback control law as follows Eq. (25)

$$u_{LQR} = -K_{LQR}x(t) \quad (25)$$

To make the state vector  $x \rightarrow 0$  so that cost function  $J$  is minimum. The cost function as follows

$$J = \int_0^{+\infty} (x^T Q x + u^T R u) dt \quad (26)$$

where  $Q = Q^T \geq 0$ , and  $R = R^T > 0$  are respectively the weight matrices for the regulation error and input values.

Because  $Q$  is symmetric, positive semi-definite matrix, we set as follows Eq. (27)

$$Q = C^T C \quad (27)$$

Assumption the pair  $(A, B)$  is stabilizable và the pair  $(A, C)$  is detectable. The optimal control is defined by Eq. (28) where

$$K_{LQR} = R^{-1} B^T S \quad (28)$$

$S$  is symmetric matrix, positive definite, and is the solution of the ARE (Algebraic Riccati Equation) in Eq. (29)

$$0 = -SA - A^T S + SBR^{-1}B^T S - Q \quad (29)$$

In this paper, weighting matrices  $Q$  and  $R$  are defined by

$$Q = \begin{bmatrix} 1 & 0 & 0 & 0 \\ 0 & 0.1 & 0 & 0 \\ 0 & 0 & 100 & 0 \\ 0 & 0 & 0 & 0.1 \end{bmatrix}, R = 0.04 \quad (30)$$

The linear feedback gain is computed by using Matlab command  $K_{LQR} = lqr(A, B, Q, R)$ . The results is given by

$$K_{LQR} = [5 \quad 3.5367 \quad 47.7315 \quad -3.3707] \quad (31)$$

#### C. CPBC-LQR

LQR is well-known control technique in the class of linear control schemes. Advantage of LQR is well-stabilizing Furuta pendulum around working point. However, their working space is just being around the working point and we do not know suitable working range of the system. Differently, nonlinear control, such as passivity-based control has a wide working range due to flexible structure of controller and stability proved by Lyapunov criteria. Hence, we propose a hybrid controller which can combine LQR and PBC to verify stabilization control of RIP at working point. The structure of hybrid control scheme CPBC-LQR is shown in Fig. 2.

Control law of hybrid control scheme CPBC-LQR is defined by combining equations (24) & (25) as

$$V_{in} = u_{PBC} + u_{LQR} = G(\theta) - K_p q - K_d \dot{q} - K_{LQR} x \quad (32)$$

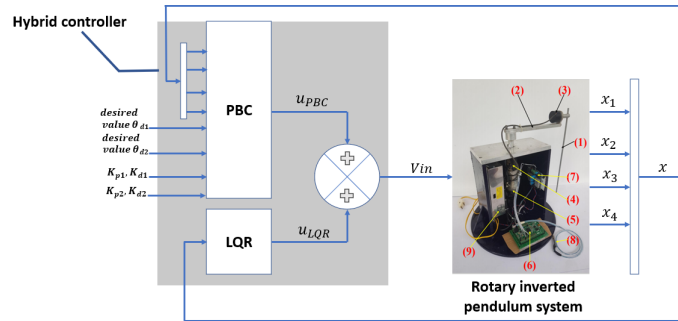


Fig. 2. Structure of hybrid control scheme CPBC-LQR.

where  $V_{in}$  is input voltage that provides for DC servo motor.

Our controller parameters are listed in Table III. Those controller parameters are chosen by try-and-error method.

TABLE III. CONTROLLER PARAMETERS

Controller parameters	Value
$K_{p1}$	4
$K_{d1}$	2.18
$K_{p2}$	5
$K_{d2}$	2
$K_{LQR}$	[5 3.5367 47.7315 -3.3707]
$\theta_{d1}$	0
$\theta_{d2}$	0

#### IV. EXPERIMENTAL PLATFORM

In this subsection, experimental test bed which is designed by authors, is shown Fig. 3. Physical RIP system has been built up and validated control approaches in many studies before [49]–[54]. The construction of experiment setup consists of:

- 1) Pendulum link
- 2) Arm link
- 3) A 500 ppr incremental pendulum encoder
- 4) DC servo motor TAMAGAWA SEIKI 24VDC - 30W
- 5) A 100 ppr incremental rotary encoder
- 6) Micro-controller STM32F407VG Discovery electronic board
- 7) Driver IR2184
- 8) Module UART CP2102
- 9) Power supplier 24VDC-10A

Besides, Waijung blockset version 17.03 has been used in work to support compilation and verification on MATLAB<sup>®</sup> 2018a. Currently, MathWorks<sup>®</sup> develops MATLAB<sup>®</sup>/Simulink<sup>®</sup> environment for STM32F4, the program files required for the embedded system are automatically created and loaded into the processor. Waijung blockset library is developed by Aimagin company that provides an option to make a Simulink-based application. The detail information of Waijung block-

set library 1 can be found at <https://waijung1.aimagin.com/>. Waijung blockset are also used in many studies such as [74]–[80]. Physical parameters of real-time experiment platform is provided in Table I.

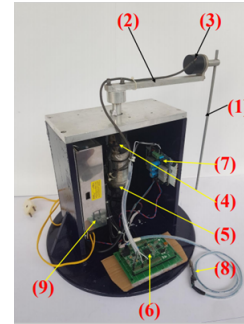


Fig. 3. Rotary inverted pendulum experimental platform.

Connection among components is shown in Fig. 4. DC motor TAMAGAWA SEIKI 24VDC-30W include an integrated 100 ppr rotary encoder for arm state measurement ( $x_3$ ). Driver IR2184 is connected with the arm motor following control command (*Volts*) generated by CPBCLQR controller. Encoder of pendulum link with 500 ppr is used to measure the pendulum state ( $x_1$ ). STM32F407VG Discovery electronic board takes responsibility for controlling the RIP with CPBCLQR, LQR control schemes.

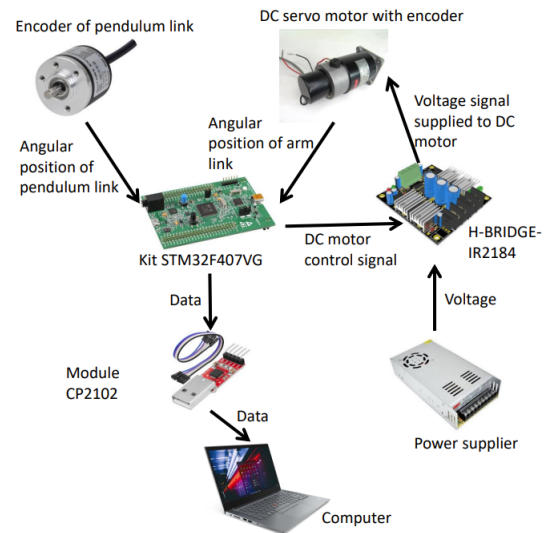


Fig. 4. Connection of components.

#### V. RESULTS

##### A. Numerical simulation results

1) *Without Disturbances*: Simulink model is shown Fig. 5 by using MATLAB/Simulink toolbox. Contents of Fig. 6 are performance of state responses of output system by implementing

CPBC-LQR. The rest of Fig. 6 is organized as follows. State response of angular position of arm  $\theta_1$  (rad), state response of angular velocity of arm  $\dot{\theta}_1$ (rad/s), state response of angular position of pendulum  $\theta_2$  (rad), state response of angular velocity of pendulum  $\dot{\theta}_2$ (rad/s), control input (V). Starting points of RIP are set up for this simulation as follows:  $x = [0.1 \ 0 \ 0.1 \ 0]$  (rad). According to the first graph of Fig. 6, the angle of pendulum is back to “0” (rad) after 1.5 seconds, maximum overshoot range of this state is  $[-0.04; 0.1]$  (rad). In the third graph, the angle of arm stabilizes at equilibrium point after 1.5 seconds and maximum overshoot range of this state is  $[-0.31; 0.1]$  (rad). Angular velocity of pendulum and arm are depicted in the second and fourth graph of this figure. Maximum overshoot range of those states are  $[-0.61; 0.2]$  (rad/s) and  $[-1.8; 0.2]$  (rad/s), respectively. Voltage input of RIP during the operation is described in the last graph. After analyzing and discussing, we observe that RIP with CPBC-LQR can stabilize at vertical upright position.

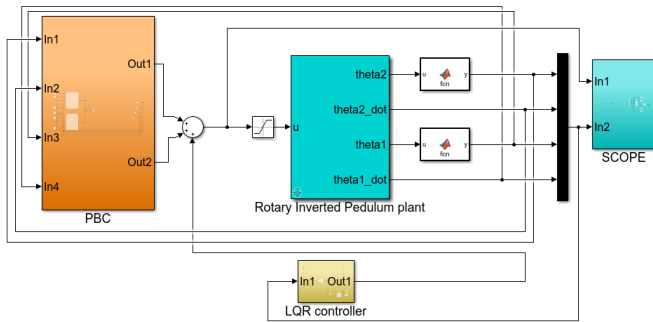


Fig. 5. Simulink model in MATLAB/Simulink in case without disturbance.

Fig. 7 delivers a comparison between performance of system with CPBC-LQR and LQR. The responses of output system by, respectively, using CPBC-LQR and conventional LQR are illustrated in Fig. 7, from which, one can get that proposed controller is fast than the one by using LQR control scheme. It can be observed that the system with CPBC-LQR has better performance, in terms of less overshoot, faster convergence in the pendulum angle, and arm angle. Angular velocity of pendulum and arm are depicted in the second and fourth graph of this figure. In the end of this figure, the control input with two controllers are also compared.

2) *With Disturbances:* In this subsection, a comparison is conducted with a pulse wise fault that affects to system at a definite time ( $t= 0.5, 1.5, 2.5, 3.5,$  and  $4.5$  seconds). Fig. 8 shows simulation model in case with disturbances. Fig. 9 delivers a comparison between performance of system with CPBC-LQR and LQR. The responses of output system by, respectively, using CPBC-LQR and conventional LQR are illustrated in Fig. 9. When being disturbed, LQR is still robust but the pendulum ( $\theta_2$ ) is varied in quite large range. At each time of pulse wise

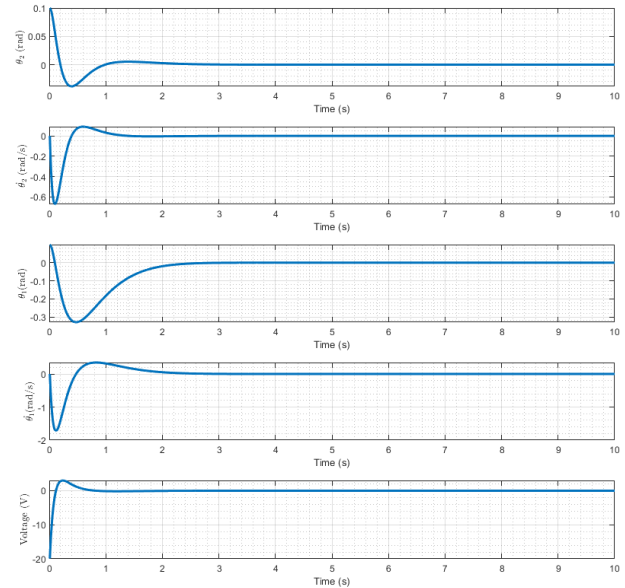


Fig. 6. State responses of output system with CPBC-LQR without disturbances.

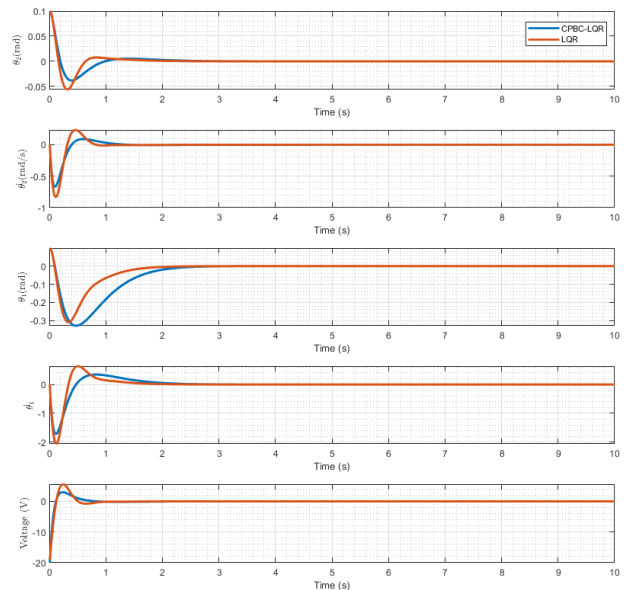


Fig. 7. Performance comparison between CPBC-LQR and LQR without disturbances.

fault impacted to the system, peak value of pendulum state of LQR controller is  $[-0.05, 0.05]$  (rad), while peak value of pendulum state of CPBCLQR controller is  $[-0.04, 0.04]$  (rad). Data shown in Fig. 9 imply that CPBCLQR provided faster responses, less settling time, and smaller overshoot as comparing to the ordinary LQR in disturbances conditions.

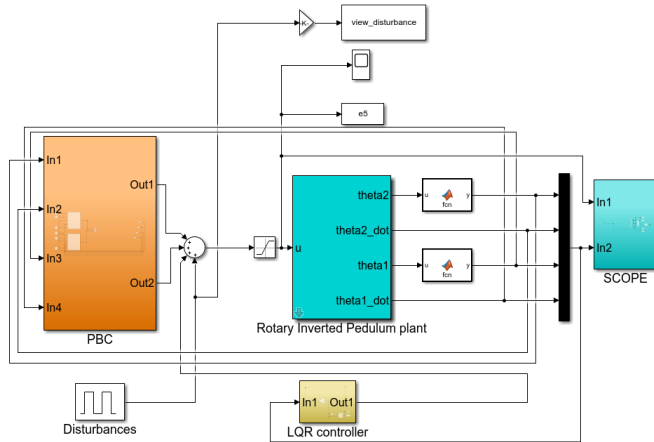


Fig. 8. Simulink model in MATLAB/Simulink in case with disturbances.

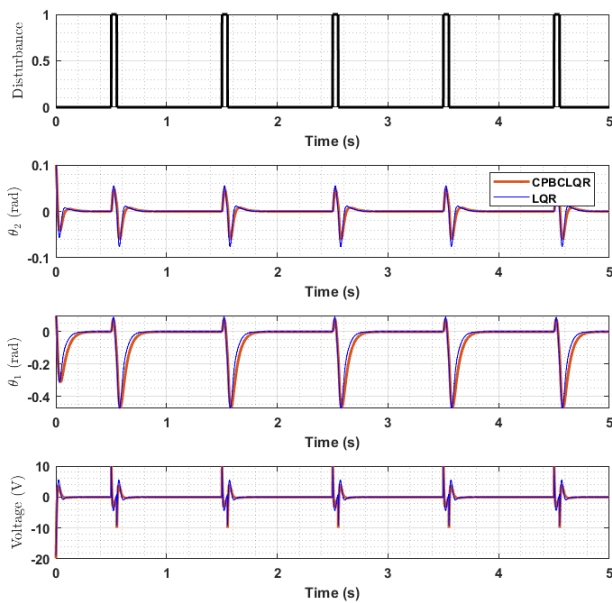


Fig. 9. Performance comparison between CPBCLQR and LQR with disturbances.

**B. Experimental results**

The main purpose of this subsection is to provide performance of state responses of output RIP via experiment. Figures

10 and 11 show two statuses of RIP. Fig. 10 shows the system is in the idle mode, i.e., the machine is ready and available, but is not doing anything productive. Fig. 10 shows the RIP is stable at equilibrium point with CPBCLQR approach. Accordingly, state responses of output can be viewed in Fig. 12



Fig. 10. Rotary inverted pendulum is in idle time.



Fig. 11. The inverted pendulum is in upright position (equilibrium point) with CPBCLQR controller which is captured from experimental video. Source: Combining Passivity-Based Control and Linear Quadratic Regulator To Control RIP. <https://www.youtube.com/shorts/JibxqHhBQA4>.

Experiment results are drawn in Fig. 12. Fig. 12 delivers the comparison between performance of system with CPBCLQR and LQR. The responses of output system by, respectively, using CPBCLQR and LQR are illustrated in Fig. 12, from which, one can get that proposed controller is fast than the one by using LQR control scheme. In the operation time, LQR is still robust but the pendulum ( $\theta_2$ ) is varied in quite larger range  $[-0.02, 0.02]$  (rad) than the CPBCLQR  $[-0.01, 0.01]$  (rad). For the rotary arm state  $\theta_1$  with LQR, we can observe that the response of arm state operates like a sine wave with oscillation amplitude is  $[-0.01, 0.31]$  (rad), while response of arm state with CPBCLQR oscillates around zero radian. It can be observed that the system with CPBCLQR has better performance, in terms of less overshoot, faster convergence in the pendulum angle, and arm angle. The angle of arm with CPBCLQR tracks equilibrium point closely, while angle of arm with LQR controller has large amplitude. Angular velocity of pendulum and arm are depicted in the second and fourth

graph of this figure. In the end of this figure, the control input with two controllers are also compared.

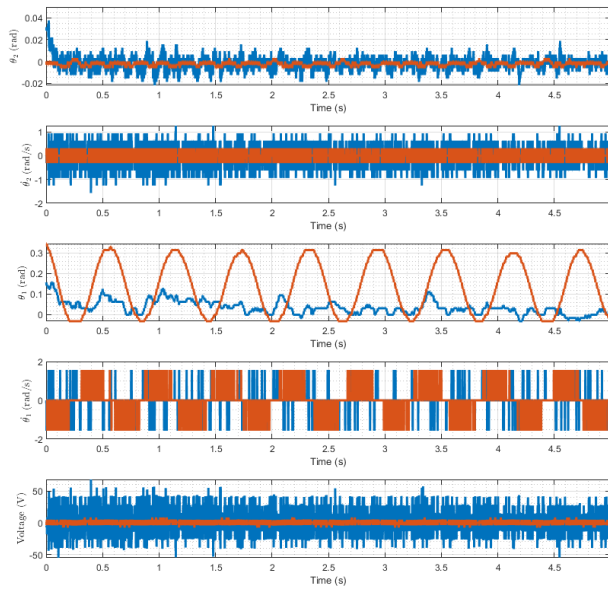


Fig. 12. State responses of output real time RIP system with CPBCLQR and LQR techniques

Video clip of the experiment can be viewed at source <https://www.youtube.com/shorts/JibxqHhBQA4> or scanned a QR code in Fig. 13. In this video, CPBC-LQR technique implemented to 2-DOF RIP for stabilization in the upright position. As it can be seen in the video clip, the CPBCLQR ensures very good performance in reality.



Fig. 13. Video clip of the experiment

## VI. CONCLUSION

In this manuscript, we have proposed a combination of passivity-based control and linear quadratic regulator for RIP system. Simulation and experiment are performed to qualify the proposed controller CPBC-LQR. Besides, comparison between CPBC-LQR and conventional LQR is carried out, analyzed, and discussed in detailed via simulation on MATLAB/Simulink

and laboratory experiment. Both simulation and experimental results show that the proposed design is able to give proper performance. The vital characteristics of CPBCLQR are effectiveness, robustness, and fast adaptation to changes of hardware. Actually, controllers parameters are defined by using try-and-error method. Accordingly, performance of CPBCLQR can be improved by using some optimization methods to optimize controller parameters such as gravity searching algorithm, genetic algorithm. This term could open a new research in the future. Additionally, we will focus on extending the proposed control scheme CPBC-LQR for complex under-actuated robot such as rotary double parallel inverted pendulum.

## ACKNOWLEDGMENT

We acknowledge the support of time and facilities from Ho Chi Minh City University of Technology (HCMUT), Viet Nam National University Ho Chi Minh City (VNUHCMC) for this study.

## CONFLICT OF INTEREST

The authors declare no conflict of interest.

## REFERENCES

- [1] F. Katsuhisa, M. Yamakita, and S. Kobayashi, "Swing-up control of inverted pendulum using pseudo-state feedback," *Proceedings of the Institution of Mechanical Engineers, Part I: Journal of Systems and Control Engineering*, vol. 206, no. 4, pp. 263-269, 2019, doi:[https://doi.org/10.1243/PIME\\_PROC\\_1992\\_206\\_341\\_02](https://doi.org/10.1243/PIME_PROC_1992_206_341_02).
- [2] K. Furuta, Y. Xu and R. Gabasov, "Computation of time optimal swing up control of single pendulum," *IECON'99. Conference Proceedings. 25th Annual Conference of the IEEE Industrial Electronics Society (Cat. No.99CH37029)*, San Jose, CA, USA, 1999, pp. 1165-1170 vol.3, doi: 10.1109/IECON.1999.819375.
- [3] J. Akesson and K. J. Astrom, "Safe manual control of the Furuta pendulum," *Proceedings of the 2001 IEEE International Conference on Control Applications (CCA'01) (Cat. No.01CH37204)*, Mexico City, Mexico, 2001, pp. 890-895, doi: 10.1109/CCA.2001.973982.
- [4] A. S. Shiriaev, L. B. Freidovich, A. Robertsson, R. Johansson and A. Sandberg, "Virtual-Holonomic-Constraints-Based Design of Stable Oscillations of Furuta Pendulum: Theory and Experiments," *IEEE Transactions on Robotics*, vol. 23, no. 4, pp. 827-832, Aug. 2007, doi: 10.1109/TRO.2007.900597.
- [5] M. Antonio-Cruz, V. M. Hernández-Guzmán and R. Silva-Ortigoza, "Limit Cycle Elimination in Inverted Pendulums: Furuta Pendulum and Pendubot," *IEEE Access*, vol. 6, pp. 30317-30332, 2018, doi: 10.1109/ACCESS.2018.2839642.
- [6] A. Wadi, J. -H. Lee and L. Romdhane, "Nonlinear sliding mode control of the Furuta pendulum," *2018 11th International Symposium on Mechatronics and its Applications (ISMA)*, Sharjah, United Arab Emirates, 2018, pp. 1-5, doi: 10.1109/ISMA.2018.8330131.
- [7] J. Xu, Y. Niu, C. -C. Lim and P. Shi, "Memory Output-Feedback Integral Sliding Mode Control for Furuta Pendulum Systems," in *IEEE Transactions on Circuits and Systems I: Regular Papers*, vol. 67, no. 6, pp. 2042-2052, June 2020, doi: 10.1109/TCSI.2020.2970090.
- [8] F. Muratore, C. Eilers, M. Gienger and J. Peters, "Data-Efficient Domain Randomization With Bayesian Optimization," *IEEE Robotics and Automation Letters*, vol. 6, no. 2, pp. 911-918, April 2021, doi: 10.1109/LRA.2021.3052391.
- [9] A. de Carvalho, J. F. Justo, B. A. Angélico, A. M. de Oliveira and J. I. da Silva Filho, "Rotary Inverted Pendulum Identification for Control by Paraconsistent Neural Network," *IEEE Access*, vol. 9, pp. 74155-74167, 2021, doi: 10.1109/ACCESS.2021.3080176.

- [10] R. R. CB, and F. M. U. de Araujo, "Lyapunov-based continuous-time nonlinear control using deep neural network applied to underactuated systems," *Engineering Applications of Artificial Intelligence*, vol. 107, pp. 357–374, 2022, doi:<https://doi.org/10.1016/j.engappai.2021.104519>.
- [11] X. Liu, X. Lu and Z. Gao, "A Deep Learning-Based Fault Diagnosis of Leader-Following Systems," in *IEEE Access*, vol. 10, pp. 18695–18706, 2022, doi: 10.1109/ACCESS.2022.3151155.
- [12] A. K. Pal and T. Nestorović, "Swing Up and Balance of an Inverted Pendulum Using Reinforced Learning Approach Coupled With a Proportional-Integral-Derivative Controller," *2022 International Conference on Electrical, Computer, Communications and Mechatronics Engineering (ICECCME)*, Maldives, Maldives, 2022, pp. 1-6, doi: 10.1109/ICECCME55909.2022.9988506.
- [13] E. Susanto, B. Rahmat and M. Ishitobi, "Stabilization of Rotary Inverted Pendulum using Proportional Derivative and Fuzzy Controls," *2022 9th International Conference on Information Technology, Computer, and Electrical Engineering (ICITACEE)*, Semarang, Indonesia, 2022, pp. 34–37, doi: 10.1109/ICITACEE55701.2022.9924142.
- [14] A. Gutarra, S. Palomino, E. J. Alegria and J. Cisneros, "Fuzzy Controller Design for Rotary Inverted Pendulum System Using Genetic Algorithms," *2022 IEEE ANDESCON*, Barranquilla, Colombia, 2022, pp. 1-6, doi: 10.1109/ANDESCON56260.2022.9989988.
- [15] M. Harati, A. A. Ghavifekr and A. R. Ghiasi, "Model Identification of Single Rotary Inverted Pendulum Using Modified Practical Swarm Optimization Algorithm," *2020 28th Iranian Conference on Electrical Engineering (ICEE)*, Tabriz, Iran, 2020, pp. 1-5, doi: 10.1109/ICEE50131.2020.9261035.
- [16] K. Nath and L. Dewan, "Heuristic optimization based choice of LQR weighting matrices for a rotary inverted pendulum," *2018 International Conference on Recent Trends in Electrical, Control and Communication (RTECC)*, Malaysia, Malaysia, 2018, pp. 269–274, doi: 10.1109/RTECC.2018.8625676.
- [17] A. Nagarajan and A. A. Victoire, "Optimization Reinforced PID-Sliding Mode Controller for Rotary Inverted Pendulum," in *IEEE Access*, vol. 11, pp. 24420–24430, 2023, doi: 10.1109/ACCESS.2023.3254591.
- [18] E. Cholodowicz and P. Orłowski, "Optimization of a fractional order controller for the Furuta pendulum with an output disturbance using a genetic algorithm," *2022 17th International Conference on Control, Automation, Robotics and Vision (ICARCV)*, Singapore, Singapore, 2022, pp. 373–379, doi: 10.1109/ICARCV57592.2022.10004289.
- [19] J. Huang, T. Zhang, Y. Fan and J. -Q. Sun, "Control of Rotary Inverted Pendulum Using Model-Free Backstepping Technique," *IEEE Access*, vol. 7, pp. 96965–96973, 2019, doi: 10.1109/ACCESS.2019.2930220.
- [20] F. F. M. El-Sousy, K. A. Alattas, O. Mofid, S. Mobayen and A. Fekih, "Robust Adaptive Super-Twisting Sliding Mode Stability Control of Underactuated Rotational Inverted Pendulum With Experimental Validation," *IEEE Access*, vol. 10, pp. 100857–100866, 2022, doi: 10.1109/ACCESS.2022.3208412.
- [21] Z. Samir, et al., "Adaptive fuzzy fast terminal sliding mode control for inverted pendulum-cart system with actuator faults," *Mathematics and Computers in Simulation*, vol. 210, pp. 207–234, 2023, doi: <https://doi.org/10.1016/j.matcom.2023.03.005>.
- [22] H. V. Nghi, D. P. Nhien, D. X. Ba, "A lqr neural network control approach for fast stabilizing rotary inverted pendulums," *International Journal of Precision Engineering and Manufacturing*, vol. 23, pp. 45–56, 2022, doi: <https://doi.org/10.1007/s12541-021-00606-x>.
- [23] C. A. Villaseñor-Rios and O. Gutierrez-Frias, "Stabilization Control of Rotary Base Inverted Pendulum by Combination of Lyapunov-base controller and Linear PD controller," *2022 8th International Conference on Control, Decision and Information Technologies (CoDIT)*, Istanbul, Turkey, 2022, pp. 141–145, doi: 10.1109/CoDIT55151.2022.9804012.
- [24] M. K. Habib and S. A. Ayankoso, "Hybrid Control of a Double Linear Inverted Pendulum using LQR-Fuzzy and LQR-PID Controllers," *2022 IEEE International Conference on Mechatronics and Automation (ICMA)*, Guilin, Guangxi, China, 2022, pp. 1784–1789, doi: 10.1109/ICMA54519.2022.9856235.
- [25] V. Kumar and R. Agarwal, "Modeling and Control of Inverted Pendulum cart system using PID-LQR based Modern Controller," *2022 IEEE Students Conference on Engineering and Systems (SCES)*, Prayagraj, India, 2022, pp. 01–05, doi: 10.1109/SCES55490.2022.9887706.
- [26] Ubaid Asif Farooqui, Dr.Chinta Mani Tiwari, "A dynamical model of a mobile inverted pendulum with linear and non linear controllers with time difference", *MSEA*, vol. 71, no. 4, pp. 1044–1062, Aug. 2022.
- [27] M. Alfian, et al, "Backstepping sliding mode control for inverted pendulum system with disturbance and parameter uncertainty," *Journal of Robotics and Control (JRC)*, vol. 3, no. 1, pp. 86–92, 2022, doi: <https://doi.org/10.18196/jrc.v3i1.12739>.
- [28] N. P. Nguyen, H. Oh, Y. Kim, J. Moon, J. Yang and W. -H. Chen, "Fuzzy-Based Super-Twisting Sliding Mode Stabilization Control for Under-Actuated Rotary Inverted Pendulum Systems," in *IEEE Access*, vol. 8, pp. 185079–185092, 2020, doi: 10.1109/ACCESS.2020.3029095.
- [29] L. Antonio, and H. Nijmeijer, "Passivity based control" in *Control Systems, Robotics And Automation*, vol. XIII, EOLSS Publications, pp. 206–226, 2009.
- [30] N. Chopra, M. Fujita, R. Ortega and M. W. Spong, "Passivity-Based Control of Robots: Theory and Examples from the Literature," in *IEEE Control Systems Magazine*, vol. 42, no. 2, pp. 63–73, April 2022, doi: 10.1109/MCS.2021.3139722.
- [31] S. Hao, Y. Yamashita, K. Kobayashi, "Robust passivity-based control design for active nonlinear suspension system," *International Journal of Robust and Nonlinear Control*, vol. 31, no. 1, pp. 373–392, 2022, doi: <https://doi.org/10.1002/rnc.5827>.
- [32] N. Moeini, M. Bahrami-Fard, M. Shahabadini, S. M. Azimi and H. Iman-Eini, "Passivity-Based Control of Single-Phase Cascaded H-Bridge Grid-Connected Photovoltaic Inverter," in *IEEE Transactions on Industrial Electronics*, vol. 70, no. 2, pp. 1512–1520, Feb. 2023, doi: 10.1109/TIE.2022.3165266.
- [33] C. Zhang, Y. Jiang, X. Xing, X. Li, C. Qin and B. Zhang, "Passivity-Based Control Method for Three-Level Photovoltaic Inverter to Mitigate Common-Mode Resonant Current," in *IEEE Transactions on Industrial Informatics*, doi: 10.1109/TII.2023.3234025.
- [34] K. Fujimoto, T. Baba, N. Sakata and I. Maruta, "A Passivity-Based Sliding Mode Controller for a Class of Electro-Mechanical Systems," in *IEEE Control Systems Letters*, vol. 6, pp. 1208–1213, 2022, doi: 10.1109/LCSYS.2021.3089541.
- [35] N. Sakata, K. Fujimoto, and I. Maruta, "New potential functions for passivity based sliding mode control," in *IFAC-PapersOnLine*, vol. 56, no. 1, pp. 150–155, 2022, doi: <https://doi.org/10.1016/j.ifacol.2023.02.026>.
- [36] W. Liu and Y. Wang, "Passivity-Based Sliding Mode Control for Lur'e Singularly Perturbed Time-Delay Systems with Input Nonlinearity," in *Circuits Syst Signal Process*, vol. 41 pp. 6007–6030, 2022, doi: <https://doi.org/10.1007/s00034-022-02086-4>.
- [37] M. B. Olyaei, M. Reza, J. Keighobadi, A. Ghanbari, and A. O. Zekiy, "Passivity-based hierarchical sliding mode control/observer of underactuated mechanical systems," in *Journal of Vibration and Control*, vol. 0, no. 0, 2022, doi: 10.1177/10775463221091035.
- [38] H. Du, C. Jing, B. Yan, and C. Liu, "Passivity-based adaptive robust super-twisting nonlinear control for electro-hydraulic system with uncertainties and disturbances," in *Mechanika / Mechanics*, vol. 29, no. 1, 2023, doi: <https://doi.org/10.5755/j02.mech.32405>.
- [39] C. Chan-Zheng, P. Borja and J. M. A. Scherpen, "Tuning of Passivity-Based Controllers for Mechanical Systems," in *IEEE Transactions on Control Systems Technology*, doi: 10.1109/TCST.2023.3260995.
- [40] A. Bakeer, M. Alhasheem and H. M. Elhelw, "Uninterruptible Power Supply: An Optimal Passivity-Based Control Scheme," *2023 IEEE Power and Energy Society Innovative Smart Grid Technologies Conference (ISGT)*, Washington, DC, USA, 2023, pp. 1–5, doi: 10.1109/ISGT51731.2023.10066406.
- [41] P. Borja, R. Ortega and J. M. A. Scherpen, "New Results on Stabilization of Port-Hamiltonian Systems via PID Passivity-Based Control," in *IEEE Transactions on Automatic Control*, vol. 66, no. 2, pp. 625–636, Feb. 2021, doi: 10.1109/TAC.2020.2986731.
- [42] M. Cucuzzella, R. Lazzari, Y. Kawano, K. C. Kosaraju and J. M. A. Scherpen, "Robust Passivity-Based Control of Boost Converters in DC Microgrids," *2019 IEEE 58th Conference on Decision and Control (CDC)*, Nice, France, 2019, pp. 8435–8440, doi: 10.1109/CDC40024.2019.9029657.
- [43] D. Handaya, R. Fauziah, "Proportional-Integral-Derivative and Linear Quadratic Regulator Control of Direct Current Motor Posi-

- tion using Multi-Turn Based on LabView,” in *Journal of Robotics and Control (JRC)*, vol. 2, no. 4, pp. 332-336, 2021, doi: <https://doi.org/10.18196/jrc.24102>.
- [44] J. Ma, Z. Cheng, X. Zhang, Z. Lin, F. L. Lewis and T. H. Lee, “Local Learning Enabled Iterative Linear Quadratic Regulator for Constrained Trajectory Planning,” in *IEEE Transactions on Neural Networks and Learning Systems*, doi: 10.1109/TNNLS.2022.3165846.
- [45] L. Ye, H. Zhu and V. Gupta, “On the Sample Complexity of Decentralized Linear Quadratic Regulator with Partially Nested Information Structure,” in *IEEE Transactions on Automatic Control*, 2022, doi: 10.1109/TAC.2022.3215940.
- [46] J. Ma, Z. Cheng, X. Li, W. Wang, M. Tomizuka and T. H. Lee, “Data-Driven Linear Quadratic Optimization for Controller Synthesis With Structural Constraints,” in *IEEE Transactions on Cybernetics*, doi: 10.1109/TCYB.2022.3233865.
- [47] Y. Yang, B. Kiumarsi, H. Modares and C. Xu, “Model-Free Policy Iteration for Discrete-Time Linear Quadratic Regulation,” in *IEEE Transactions on Neural Networks and Learning Systems*, vol. 34, no. 2, pp. 635-649, Feb. 2023, doi: 10.1109/TNNLS.2021.3098985.
- [48] X. Yang and X. Zheng, “Swing-Up and Stabilization Control Design for an Underactuated Rotary Inverted Pendulum System: Theory and Experiments,” in *IEEE Transactions on Industrial Electronics*, vol. 65, no. 9, pp. 7229-7238, Sept. 2018, doi: 10.1109/TIE.2018.2793214.
- [49] M. Švec, Š. Ileš and J. Matuško, “Sliding Mode Control of Custom Built Rotary Inverted Pendulum,” *2020 43rd International Convention on Information, Communication and Electronic Technology (MIPRO)*, Opatjija, Croatia, 2020, pp. 943-947, doi: 10.23919/MIPRO48935.2020.9245135.
- [50] T. T. Sarkar, L. Dewan and C. Mahanta, “Real Time Swing up and Stabilization of Rotary Inverted Pendulum System,” *2020 International Conference on Computational Performance Evaluation (ComPE)*, Shillong, India, 2020, pp. 517-522, doi: 10.1109/ComPE49325.2020.9200152.
- [51] B. Sütő and Z. Lendek, “Switching control of a rotary inverted pendulum,” *2022 26th International Conference on System Theory, Control and Computing (ICSTCC)*, Sinaia, Romania, 2022, pp. 111-116, doi: 10.1109/ICSTCC55426.2022.9931817.
- [52] R. Ganganath, C. Ranganath and B. Annasiwaththa, “Remotely Operated Rotary Inverted Pendulum System for Online Control Engineering Education,” *2022 3rd International Conference on Electrical Engineering and Informatics (Icon EEI)*, Pekanbaru, Indonesia, 2022, pp. 137-142, doi: 10.1109/IconEEI55709.2022.9972285.
- [53] Z. B. Hazem and Z. Bingül, “Comprehensive Review of Different Pendulum Structures in Engineering Applications,” in *IEEE Access*, vol. 11, pp. 42862-42880, 2023, doi: 10.1109/ACCESS.2023.3269580.
- [54] H. -R. Li, Z. -Y. Nie, E. -Z. Zhu, W. -X. He and Y. -M. Zheng, “Double Loop DR-PID Control of A Rotary Inverted Pendulum,” *2021 IEEE International Conference on Networking, Sensing and Control (ICNSC)*, Xiamen, China, 2021, pp. 1-5, doi: 10.1109/ICNSC52481.2021.9702192.
- [55] M. Ryalat and D. S. Laila, “IDA-PBC for a class of underactuated mechanical systems with application to a rotary inverted pendulum,” *52nd IEEE Conference on Decision and Control*, Firenze, Italy, 2013, pp. 5240-5245, doi: 10.1109/CDC.2013.6760713.
- [56] Y. Xu, M. Iwase, and K. Furuta, “Time optimal swing-up control of single pendulum,” *Journal of Dynamic Systems, Measurement and Control, Transactions of the ASME*, vol. 123, no. 3, pp. 518-527, 2001, doi: 10.1115/1.1383027.
- [57] K. Furuta and M. Iwase, “An adaptive swing-up sliding mode controller design for a real inverted pendulum system based on Culture-Bees algorithm,” *European Journal of Control*, vol. 49, no. 3, pp. 45-56, 2019, <https://doi.org/10.1016/j.ejcon.2018.12.001>.
- [58] M. Iwase, K.J. Astrom, K. Furuta, and J. Akesson, “Analysis of safe manual control by using Furuta pendulum,” in *Proceedings of the IEEE International Conference on Control Applications (CCA '06)*, pp. 568-572, October 2006, doi: 10.1109/CACSD-CCA-ISIC.2006.4776708.
- [59] V.-A. Nguyen, D.-B. Pham, D.-T. Pham, N.-T. Bui, and Q. T. Dao, “A Hybrid Energy Sliding Mode Controller for the Rotary Inverted Pendulum,” in *Lecture notes in networks and systems*, Springer International Publishing, 2022, pp. 34-41, doi: 10.1007/978-3-031-22200-9-4.
- [60] N. Bu and X. Wang, “Swing-up design of double inverted pendulum by using passive control method based on operator theory,” *International Journal of Advanced Mechatronic Systems*, vol. 10, no. 1, p. 1, Jan. 2023, doi: 10.1504/ijamechs.2023.128154.
- [61] A. Jain, A. Sharma, V. Jatly, B. Azzopardi and S. Choudhury, “Real-Time Swing-Up Control of Non-Linear Inverted Pendulum Using Lyapunov Based Optimized Fuzzy Logic Control,” in *IEEE Access*, vol. 9, pp. 50715-50726, 2021, doi: 10.1109/ACCESS.2021.3058645.
- [62] M. Abdullah, A. A. Amin, S. Iqbal, and K. Mahmood-Ul-Hasan, “Swing up and stabilization control of rotary inverted pendulum based on energy balance, fuzzy logic, and LQR controllers,” *Measurement and Control*, vol. 54, no. 9-10, pp. 1356-1370, Nov. 2021, doi: 10.1177/00202940211035406.
- [63] E. Susanto, A. Surya Wibowo and E. Ghiffary Rachman, “Fuzzy Swing Up Control and Optimal State Feedback Stabilization for Self-Erecting Inverted Pendulum,” in *IEEE Access*, vol. 8, pp. 6496-6504, 2020, doi: 10.1109/ACCESS.2019.2963399.
- [64] I. Chawla and A. Singla, “Real-Time Stabilization Control of a Rotary Inverted Pendulum Using LQR-Based Sliding Mode Controller,” *Arabian Journal for Science and Engineering*, vol. 46, no. 3, pp. 2589-2596, Mar. 2021, doi: 10.1007/s13369-020-05161-7.
- [65] A. De Carvalho, B. A. Angelico, J. F. Justo, A. M. De Oliveira, and J. I. Da Silva Filho, “Model reference control by recurrent neural network built with paraconsistent neurons for trajectory tracking of a rotary inverted pendulum,” *Applied Soft Computing*, vol. 133, p. 109927, Jan. 2023, doi: 10.1016/j.asoc.2022.109927.
- [66] N. Gupta and L. Dewan, “Trajectory Tracking And Balancing Control Of Rotary Inverted Pendulum System Using Quasi-Sliding Mode Control, 1-8,” *Mechatronic Systems and Control*, vol. 50, no. 1, Jan. 2022, doi: 10.2316/j.2022.201-0231.
- [67] J. Montoya-Cháirez, J. Moreno-Valenzuela, V. Santibáñez, R. Carelli, F. G. Rossomando, and R. Pérez-Alcocer, “Combined adaptive neural network and regressor-based trajectory tracking control of flexible joint robots,” *Iet Control Theory and Applications*, vol. 16, no. 1, pp. 31-50, Oct. 2021, doi: 10.1049/cth2.12202.
- [68] C. Eilers, J. Eschmann, R. Menzenbach, B. Belousov, F. Muratore and J. Peters, “Underactuated Waypoint Trajectory Optimization for Light Painting Photography,” *2020 IEEE International Conference on Robotics and Automation (ICRA)*, Paris, France, 2020, pp. 1505-1510, doi: 10.1109/ICRA40945.2020.9196516.
- [69] K. Albert, K. S. Phogat, F. Anhalt, R. N. Banavar, D. Chatterjee and B. Lohmann, “Structure-Preserving Constrained Optimal Trajectory Planning of a Wheeled Inverted Pendulum,” in *IEEE Transactions on Robotics*, vol. 36, no. 3, pp. 910-923, June 2020, doi: 10.1109/TRO.2020.2985579.
- [70] S. Howimanporn, S. Chookaew and C. Silawatchananai, “Comparison between PID and Sliding Mode Controllers for Rotary Inverted Pendulum Using PLC,” *2020 4th International Conference on Automation, Control and Robots (ICACR)*, Rome, Italy, 2020, pp. 122-126, doi: 10.1109/ICACR51161.2020.9265510.
- [71] G. Demirkiran, Ö. Erdener, Ö. Akpınar, P. Demirtaş, M. Y. Arık and E. Güler, “Control of an Inverted Pendulum by Reinforcement Learning Method in PLC Environment,” *2020 Innovations in Intelligent Systems and Applications Conference (ASYU)*, Istanbul, Turkey, 2020, pp. 1-5, doi: 10.1109/ASYU50717.2020.9259890.
- [72] R. Hernández Ronald, A. Bastidas Alejandra, R. Calderon Jaime and T. B. José Antonio, “PI tuning based on Bacterial Foraging Algorithm for flow control,” *2020 IX International Congress of Mechatronics Engineering and Automation (CIIMA)*, Cartagena, Colombia, 2020, pp. 1-6, doi: 10.1109/CIIMA50553.2020.9290289.
- [73] L. Rónai and T. Szabó, “Application of Rexroth Controlling for Inverted Pendulum,” *International Journal of Engineering and Management Sciences*, vol. 4, no. 1, pp. 174-179, <https://doi.org/10.21791/IJEMS.2019.1.22>.
- [74] J. A. Reshi and R. K, “A Novel Logical Band Approach for BLDC Motor Speed Control,” *2022 1st International Conference on Sustainable Technology for Power and Energy Systems (STPES)*, SRINAGAR, India, 2022, pp. 1-6, doi: 10.1109/STPES54845.2022.10006435.
- [75] A. V. Vyngra, S. G. Chernyi and S. S. Sokolov, “Development an Active Filter Control Software with the Addition of Algorithms for

- Working at Perturbations,” *2022 Conference of Russian Young Researchers in Electrical and Electronic Engineering (ElConRus)*, Saint Petersburg, Russian Federation, 2022, pp. 497-499, doi: 10.1109/ElConRus54750.2022.9755540.
- [76] I. Polyuschenkov, “Development of Double-motor Electric Drive for Screen Wipers,” *2022 29th International Workshop on Electric Drives: Advances in Power Electronics for Electric Drives (IWED)*, Moscow, Russian Federation, 2022, pp. 1-6, doi: 10.1109/IWED54598.2022.9722590.
- [77] D. Tristán-Rodríguez, R. Garrido and E. Mezura-Montesb, “Optimization of a state feedback controller using a PSO algorithm,” *2022 IEEE 18th International Conference on Automation Science and Engineering (CASE)*, Mexico City, Mexico, 2022, pp. 729-734, doi: 10.1109/CASE49997.2022.9926501.
- [78] G. Hernández-Melgarejo, A. Luviano-Juárez and R. Q. Fuentes-Aguilar, “A Framework to Model and Control the State of Presence in Virtual Reality Systems,” in *IEEE Transactions on Affective Computing*, vol. 13, no. 4, pp. 1854-1867, 1 Oct.-Dec. 2022, doi: 10.1109/TAFFC.2022.3195697.
- [79] K. S et al., “Torque control-based induction motor speed control using Anticipating Power Impulse Technique,” *The International Journal of Advanced Manufacturing Technology*, pp. 1-9, Feb. 2023, doi: 10.1007/s00170-023-10893-5.
- [80] B. Mirac and A. Kilic, “Assessment of Several PID Controllers Applied to DC Motors,” *2021 5th International Symposium on Multidisciplinary Studies and Innovative Technologies (ISMSIT)*, Ankara, Turkey, 2021, pp. 700-705, doi: 10.1109/ISMSIT52890.2021.9604632.
- [81] M. T. Vo, “Back-stepping control for rotary inverted pendulum,” *Journal of Technical Education Science*, no. 59, pp. 93–101, Aug. 2020, doi: <https://jte.edu.vn/index.php/jte/article/view/110>.